Renewable Energy 245 (2025) 122848

Contents lists available at ScienceDirect

Renewable Energy

journal homepage: www.elsevier.com/locate/renene

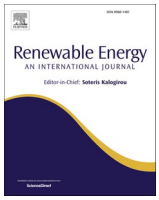

Facile polymer-based monolithic microbial fuel cells

Vikash Kumar, Sarat Singamneni *

Additive Manufacturing Research Centre, Auckland University of Technology Auckland, New Zealand

ARTICLE INFO

Keywords:
Microbial fuel cell
3D printing
Porolay
Bacteria
Electric paint

ABSTRACT

Additive manufacturing technologies have shown promising results over conventional methods in fabricating all components of energy devices. A relentless drive to fabricate all critical components in a single step is the core driving force. In the current work, monolithic microbial fuel cells (MFCs) are evaluated using Porolay series filaments, replacing multilayer cellulose paper substrates-based MFCs for the first time. Leveraging the benefits of 3D printing, different filaments of the Porolay series are employed for varying the thickness and internal architectures of critical components such as membranes, electrodes and reservoirs, targeting the maximum throughput. Amongst four different filaments, the Gel lay performed the best in terms of power output. The optimised thicknesses are membrane 0.4 mm, reservoir 1 mm, and layer above reservoir 0.6 mm. Further, facile electrodes are developed, combining screen printing and drop casting using an electric paint, which covers the surface as well as the internal strands of the printed substrate, enhancing the electron-capturing sites. Based on the optimised critical components and filaments, the monolithic printed substrate is able to generate a stable OCV of 0.49 V for approximately 90 min and deliver a power of 12.3 μW/cm^2 using E. Coli as the biocatalyst. This low-cost device can assist point-of-care testing as a freestanding power source.

1. Introduction

Microbial Fuel cells (MFCs) are gaining popularity as a green technology as they generate power from organic waste materials. Microbial fuel cells are based on the bio-electrochemical process where the reactor consists of an anode and cathode, which are separated by a proton exchange membrane. On the anode side, degradation of organic waste materials occurs through an oxidation process, whereby electrons are generated. These generated electrons travel to the cathode side via an external load, thus completing the circuit [1]. In the era of miniaturisation, there is a growing need to develop miniaturised MFCs using the microfabrication process. Miniaturised MFCs offer several benefits, such as low cost, quick power generation, powering portable devices, high power density, low internal resistance, and being stand-alone and self-sustaining devices [2]. Despite these benefits, they are not used in practical applications yet due to several issues. First, MFCs possess complicated configurations of parts such as anode, cathode, gasket, ion exchange, casing, microvalve, micropump, and the need for external power for driving the fluids, which is much higher than the power generated from the MFC itself. Furthermore, the cost of fabrication of ion exchange membranes is high, and their assembly with other parts is cumbersome and hinders batch production. Moreover, clamping and bonding each functional component is challenging where any lack of quality may result in the development of internal resistance. In addition, these small-scale MFCs require several hours to days to acclimate microorganisms on the anode. Numerous investigations have been conducted to improve the power output by employing different configurations, membranes, and redox mediators, which make the devices bulky and costly. There is a need to develop a user-friendly, cost-effective, facile fabrication process.

Paper-based MFCs have attained growing interest recently due to low cost, rapid design, and fabrication. The capillary behaviour of the paper makes it suitable for self-powered fluid transport, alleviating the need for a microvalve or pump. The paper-based MFCs render rapid adsorption of microbes and promote the bacterial cells to adhere to the electrode quickly, leading to faster electron transfer from bacterial respiration [3]. Paper-based devices promote good coherence with a large number of chemicals and bioreagents and offer potential other qualities such as easy disposal, lightweight, flexible, biocompatible, and high surface-to-volume ratio, which make them suitable for disposable paper-based lab-on-chip (LOC) devices for rapid point-of-care diagnostics and real-time monitoring of patients [4]. The miniaturised Microfluidic paper-based analytical device for biofuel cells (μPAD-BFC) and powering ultra-low-power wireless sensors is another prominent

* Corresponding author. Auckland University of Technology, Auckland, New Zealand.
E-mail address: sarat.singamneni@aut.ac.nz (S. Singamneni).

https://doi.org/10.1016/j.renene.2025.122848
Received 16 January 2025; Received in revised form 5 March 2025; Accepted 7 March 2025
Available online 11 March 2025

application of paper-based devices.

Veerubhotla, Das, and Pradhan developed MFCs based on Whatman filter papers that yielded 12.5 W/m^3 power. Further, paper-based anodes and cathodes were prepared using commercially available eyeliners, such as conductive ink, without any binder [5]. Jayapriya et al. [6] developed a cheap, facile technique for making conductive electrodes using CNT solution for MFCs application and were able to generate Open Circuit-voltage (OCV) of 410 mV with a peak power density (PPD) of 192 μW/cm^2, with series and 1.175 V and PPD of 15.9 mW/cm^2 in parallel mode. Jayapiriya and Goel [7] developed a cost-effective coin-sized paper-based MFC that can generate a PPD of 11.8 μW/cm^2 using E. Coli as a biocatalyst. Further, six different grades of cellulose filter papers based on pore size and thickness were used as separators. Guan et al. [8] enhanced microbial immobilisation, so the biofilm formation on carbon paper anode employing zero-dimension nitrogen-doped carbon dots as biocompatible efficient modifiers. The as-developed anode generated a power output 1.1 times higher than the counterpart raw carbon paper. Stacking was done to achieve enough OCV and PPD for practical applications. The Origami technique is one such process where individual cells are stacked in series and parallel cells [9]. Fraiwan and Choi [10] introduced the fusion concept of origami and paper-based MFC technology. A T-shaped filter paper was folded three times to connect four MFCs in series, which generated a PPD of 1.2 μW/cm^2. Mohammadifar et al. developed low-cost origami-inspired 3D microbial fuel cells using 2-D MFCs integrating anode, reservoir, cation-exchange membrane and air-cathode. In this investigation, four different anode materials for paper-based MFCs were prepared: (i) composite graphite particle/PAA (poly (amic) acid), (ii) composite graphite particle/40 % PTFE (Polytetrafluoroethylene), (iii) graphite ink with AC, and (iv) graphite ink alone [2]. Rewatkar et al. [11] developed Microfluidic paper-based microbial fuel cells (μP-MFCs) based on an origami array with customised electrode printing using an inkjet printer. Further, the printed electrode was coated with optimised MnO_2 nanoparticles as a catalyst to enhance power conversion efficiency. The origami-based two parallel connected MFCs generated OCV 0.534 V with PPD 15.9 μW/cm^2.

There has also been considerable research interest in the device design, inoculum media, electrode materials, and anolytes and catholytes. Additionally, most of the research articles incorporated different forms of cellulose paper as substrate materials for the critical components of MFCs, such as separators, reservoirs, catalysts, and electrodes, in the context of flexible electronics. Although paper-based substrates offer several benefits, they are highly fragile, with limitations on the shape, size, thickness and opportunities for customisation of properties. The limited thickness of the paper renders lesser capability of storing inoculum/cultured media, which eventually affects the PPD and OCV responses. Further, a polymer-based separator is proven to block oxygen and have better proton-exchanging properties than a paper-based counterpart. Drop casting or screen-printing methods are generally used for catalyst or electrode preparation on paper substrates, with limited properties. Evidently, there is a great scope for improving the fabrication processes, targeting better surface area for a given volume and, eventually, more reaction sites.

Based on the foregoing discussion, it is clear that a reliable and versatile manufacturing process is needed to fabricate substrates which are better than the cellulose-based paper substrates for MFCs. Polymer-based substrates could be an option considering low costs, better longevity, and ready availability. However, most polymers do not support wicking and capillary properties, which are essential aspects of self-powering MFCs. Porolay series filament is a foamy polymer that develops porosity once soaked in water for 48 h or more. This is composed of rubber-elastomeric polymer and Polyvinyl Alcohol (PVA). Post-printing, soaking, and rinsing in water will allow the PVA to dissolve and leave the structure porous. Oberoi et al. [12] utilised Lay-Fomm material for drug delivery and its impact on oral cells. Various other Lay-Fomm applications include Tissue engineering [13], biocompatible polymer materials [14], Microfluidic fuel cell channels [15], and low-cost, customised shape sorbents [16].

Once Lay-Fomm is employed as a substrate material for the critical components of MFCs, such as separator, reservoir, catalyst, and electrodes, other constraints, such as achieving different shapes and size distribution of the porosity of the substrates, should be overcome. A separator should block the flow of the inoculum medium, thus requiring a dense structure for the substrates while also allowing positive ions to pass through to the cathode side. Contrary to this, reservoir substrates are expected to hold large amounts of inoculum media, thereby needing highly porous structures. Eventually, the catalyst and electrode components need very fine pore density in a given volume, to achieve more reaction sites and better capacity to capture charge ions, as well as the throughput. All these conditions can only be met with a fabrication process that is highly flexible fabrication process.

Additive manufacturing comes in as a possible solution here, as: *(i)* The paper option can be replaced by thin-layer polymer as substrates constructed by 3D printing, *(ii)* Lay-Fomm filament materials can be evaluated as options for the substrates, *(iii)* functionally graded and controlled porosity can be targeted in the substrate structures for closely controlling critical components property, *(iv)* more importantly, substrates can be designed and developed by suitably altering the raster paths of the construction of layers in the 3D printing process, thereby targeting better power densities and voltages. Accordingly, different Poro-lay series filaments, such as Lay-Fomm 60, Lay-Fomm 40, Gel-Lay, and Lay-Felt, are employed in the current study as substrate materials for different critical components of polymer-based MFCs such as anode, cathode, reservoir and membrane, utilising the Fused Filament Fabrication (FFF) printing as a fabrication route. Further, all the critical components are printed monolithically within a single printing set-up with optimised process parameters. Conductive paint is employed to develop the anode and cathode, and manganese oxide (MnO_2) solution is used as a cathode catalyst. Lastly, material and electrochemical characterisations and optimisations for the layer thickness of critical components are done to improve the output performance of microbial biofuel cells.

2. Materials and methods

Different grades of Poro-lay series filaments, such as Lay-Fomm 60, Lay-Fomm 40, Lay-Felt, and Gel-Lay (MatterHackers, US), were evaluated as replacements for replacing the earlier paper-based substrates. The critical components of MFC, such as the electrodes, substrates, reservoir, and ion exchange membrane, were fabricated using these alternative materials. Electric paint (Bare Conductive, UK) was used without any further modification for the cathode and anode surfaces using the screen-printing method. Manganese oxide nanoparticles were used as a cathodic catalyst (purchased from Nano Research Lab, India). An electrical contact was developed using a nano silver conducting paste (purchased from Nano Research Lab, India) and used without any further modification. The *E. Coli* bacterial culture was procured from the Microbiology lab of the Auckland University of Technology, NZ. Luria-Bertani (LB) media broth was purchased from Sigma-Aldrich, NZ. All the reagents were prepared in Ultra-pure 18.2 MΩ.cm Milli-Q water.

Porolay line consists of four different types of filaments: Lay fomm 40, Lay fomm 60, Lay felt, and Gel lay. The first three have a foamy appearance, and the last one is gelatinous. Gel-Lay filament consists of a mixture of a Polyvinyl Alcohol (PVA) and elastomeric rubber polymer. Therefore, part of this strand is water soluble. After rinsing the material in water, the PVA component is dissolved, and the rubber polymer remains a micro-porous appearance. The functional component (backbone material) which gives each filament its unique features is polyurethane for Lay-form and polyamide for Gel lay, respectively. The functional component of Lay felt is rubber-elastomeric polymer, and the exact components are unknown, considering the proprietary nature of the materials. Lay fomm 40 is soft compared to Lay fomm 60, and it is

named because of the shore hardness A40 and A60, respectively.

2.1. Electrode fabrication

The substrate of 20 × 20 area and 2 mm thickness is designed using SolidWorks (R2 2023), the segmented view of different critical components, which are shown in Fig. 1. Further, a perforated plate on the cathode side allows oxygen from the air, and the top solid block protects oxygen interaction with the anode. A hole in the middle allows direct passage of the culture media to the reservoir. The optimum thickness of the membrane and the reservoir are 0.4 mm and 1 mm, respectively, and that of the plate covering reservoir is 0.6 mm. The CAD model is exported to simplify 3D for slicing before printing. The printing parameters set in the slicer are shown in Table 1.

Once the substrate is printed with different components, the next step is to develop electrodes on the printed substrates. The area of the anodic and cathodic layers is 1 × 1 cm^2 each. For the anode and the cathode, the screen coating method is applied using electric paint, which offers a sheet resistance of 55 Ω/sq at 50-μm film thickness. Once the required dimension is developed, this coating is left to dry for 12 h at ambient conditions to dry [17]. Further, the drop-casting method is deployed to coat the internal porous structure of the printed substrates. For this, a conductive paint solution with a concentration of 3 mg/ml in DI water is used, as this conductive paint is readily soluble. This resultant homogenous solution is used for depositing conductive layers (electric paint) on the anode side of the printed polymer substrate. The layer height of depositing conductive layers and internal porous coated architecture of printed polymer substrates is done by cross-section Scanning Electron Microscopy (SEM) images taken using a Field Emission Scanning Electron Microscope (FESEM, Hitachi SU-70). Next, enhancement of the cathodic property, which eventually decides the throughput, is done by dispersing 10 μl of manganese oxide (MnO_2) nanoparticles solution on dried electric paint. MnO_2 solution is prepared by dispersing in ethanol (1 mg/ml), as mentioned by Jayapiriya et al. [6]. The electrical connections are made using silver conductive paste on the anode and cathode sides. Finally, a support case is 3D-printed using PLA material for the anode and cathode side. For the anode side, a solid plate case is printed with a small hole in the middle for bacterial feed and a small square blank on the side edge for electrical connection. Similarly, a perforated plate case is 3D printed for the cathode side, allowing interaction with oxygen from the atmosphere, and a small square blank on the side edge for electrical connection. Final MFC substates after electrical paint coating and MnO_2 dispersing on the cathode side with electrical contact are shown in Fig. 2.

Table 1
3D printing parameters for printing substrates.

Parameters	Value
Layer height	0.1 mm
Layer width	0.4 mm
Top solid layers	6
Bottom solid layer	4
Infill percentage	100 %
Infill pattern	Rectilinear (0 and 90° alternate)
Printing speed	30 mm/s
Nozzle temperature	220° C

2.2. Bacterial inoculum

The *E. coli* bacterial culture is prepared in the Luria Bertani (LB) broth, comprising 10 g tryptone, 5 g yeast, and 10 g NaCl, following the protocol as described by Jayapiriya and Goel [18]. The measured OD confirmed positive inoculation of *E. coli* bacteria in the media. This inoculated bacterial culture is used as the fuel for the developed MFC modules.

2.3. Electrochemical measurement setup

The power output of the MFCs is monitored continuously in real-time in volts (V) using a Data Logger Picolog 1216 (Pico Technology Ltd., UK). Polarisation measurements are carried out using an automated computer-controlled variable resistor system. A total of resistance values, starting from 50 kΩ down to 10 Ω, are applied for 2 min each after the MFCs established steady-state open circuit voltages at the start of the experiment [19,20].

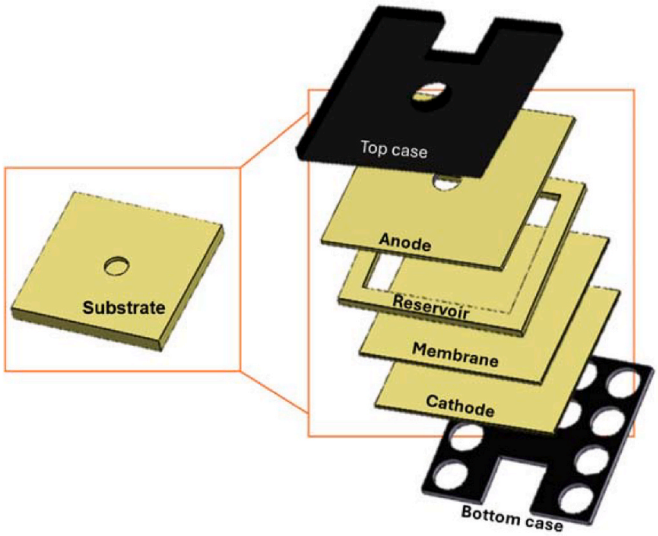

Fig. 1. Schematic diagram of substrates used in MFC with the critical parts segmented and shown as top solid plate, anode, reservoir, membrane, cathode and bottom perforated plate.

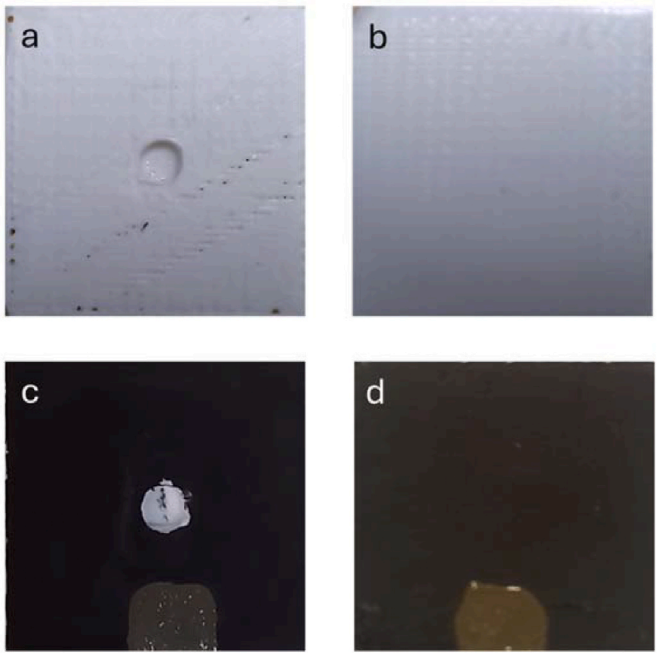

Fig. 2. Printed and water-soaked substrates (a) top view anode side, (b) bottom view cathode side, (c) Electric paint coating on anode side as well as silver layer coating for electrical contact, (d) Electric paint coating on the cathode side followed by drop casting of MnO_2 solution and silver layer coating.

3. Results and discussions

3.1. Physicochemical characterisation

The morphologies of the coating of electric paint on the anode and electric paint and MnO_2 on the cathode side are assessed using scanning electron microscopy (SEM) images. The homogeneous and uniform deposition of the electric paint on the anode side and MnO_2 on the cathode side are confirmed by Fig. 3(a) and (b), respectively. Fig. 3 (c) shows a cross-sectional view of the anode where the average thickness of electric paint coating is 10 μm.

The formation of bacterial biofilm on the anode substrate after completing the three cycles is shown in Fig. 3 (d), which shows that Porolay series filaments are biocompatible materials [21], apart from supporting the electric paint coating. EDX analysis results of Fig. 4 clearly depict that an electric paint-coated anode has a high carbon content (87.36 %), whereas in the case of the electric paint cum MnO_2-coated cathode, the carbon content dropped to 39.75 % with an increase in the Manganese content of 16.09 % as well as the Oxygen percentage [22]. Further, the tabular form displays the EDX mapping on the spatial distribution of elements in the electrode-coated printed substrates. Although the aggregation of Manganese can be seen in a few locations, it is still evenly distributed throughout the cathode, upon careful investigation. Furthermore, a high percentage of Oxygen is observed in the spectrum, which might be due to the interaction of beams with the substrate material. Polyamide is the backbone of the Gel lay, where amide groups (CO-NH) connect the repeating units in a molecular chain, and the presence of oxygen in the group could be the plausible reason for increasing the percentage [23].

3.2. Electrochemical characterisation

3.2.1. Polarisation performance

The critical parameters in monolithic polymer printed MFCs are their critical component architecture and thickness. Initial trials are performed with a thinner membrane (less than 0.4 mm), which shows layers peeling from the reservoir while removed from the printing bed. Additionally, if membrane thickness is less than 0.4 mm, it might cause cross-flow of culture to the cathode side and eventually deteriorate the performance. Further, printing density is kept at 100 %, as the soaking of the printed sample in water dissolves PVA and develops porosity. So, an initial porous setup might allow the culture to flow to the other side. Lastly, the top and bottom layers are made 100 % dense, which allows a homogeneous coating of the electrode. Some of the initial failure attempts before optimising the printing parameters are shown in Supplementary Fig. S1.

Additionally, other trials are carried out by varying the thickness of the membrane (below the reservoir) and anode thickness (above the reservoir, called anode thickness) to evaluate the performance output in terms of open circuit voltage (OCV). The trials started with Gel lay filament, keeping the membrane thickness of 0.8 mm and the anode thickness of 0.8 mm, which leads to the reservoir thickness of 0.4 mm (the total thickness of the substrate is kept at 2 mm). The maximum OCV obtained for this setup is 0.25 V for three cycles, as shown in Supplementary Fig. S2. Another setup is made with a reduced membrane thickness of 0.6 mm and reduced anode thickness of 0.6 mm, and the maximum OCV obtained for this setup is 0.28 V for three cycles, as shown in Supplementary Fig. S2. One of the reasons for this improved performance is that a thinner membrane allows more ions to transfer to the cathode side and reduces internal resistance [6]. Another reason is that a thinner anode substrate reduces the distance between inoculum storage and allows more interaction of the electrode with bacterial inoculum, eventually resulting in better performance. This result

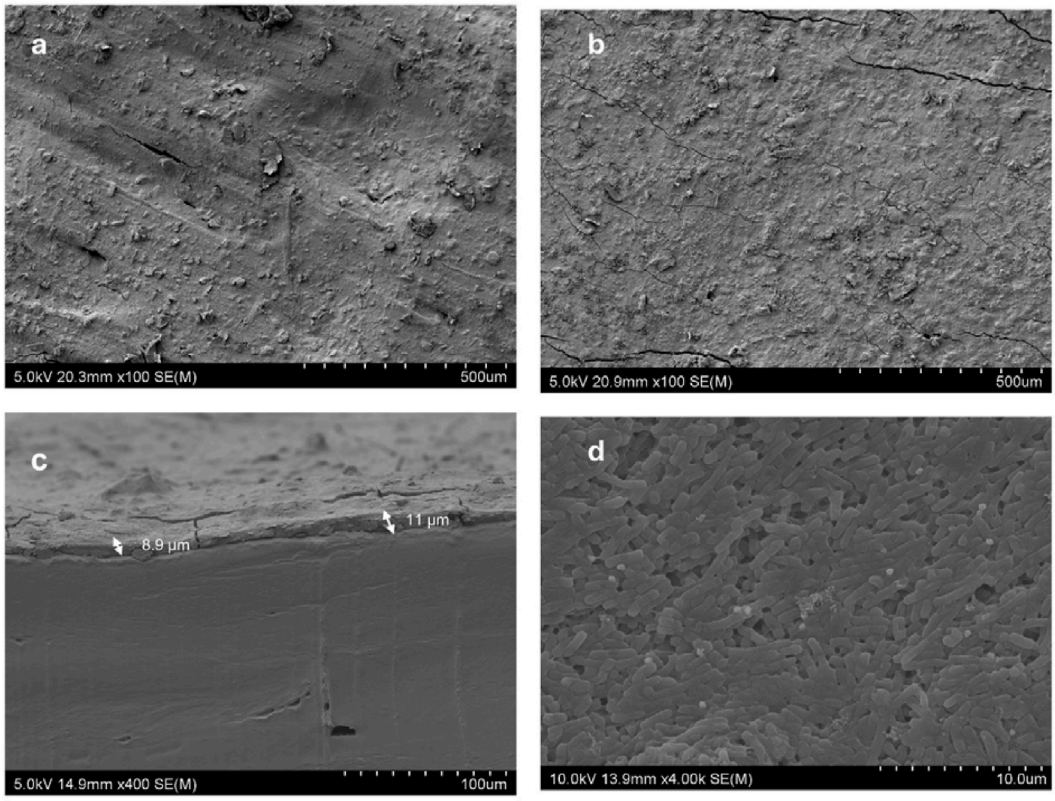

Fig. 3. Surface morphologies of (a) electric paint-coated printed anode, (b) electric paint coated with MnO_2 on the printed cathode, (c) Cross-sectional view of anode showing electric paint of average thickness 10 μm, and (d) Bacterial biofilm on the anode.

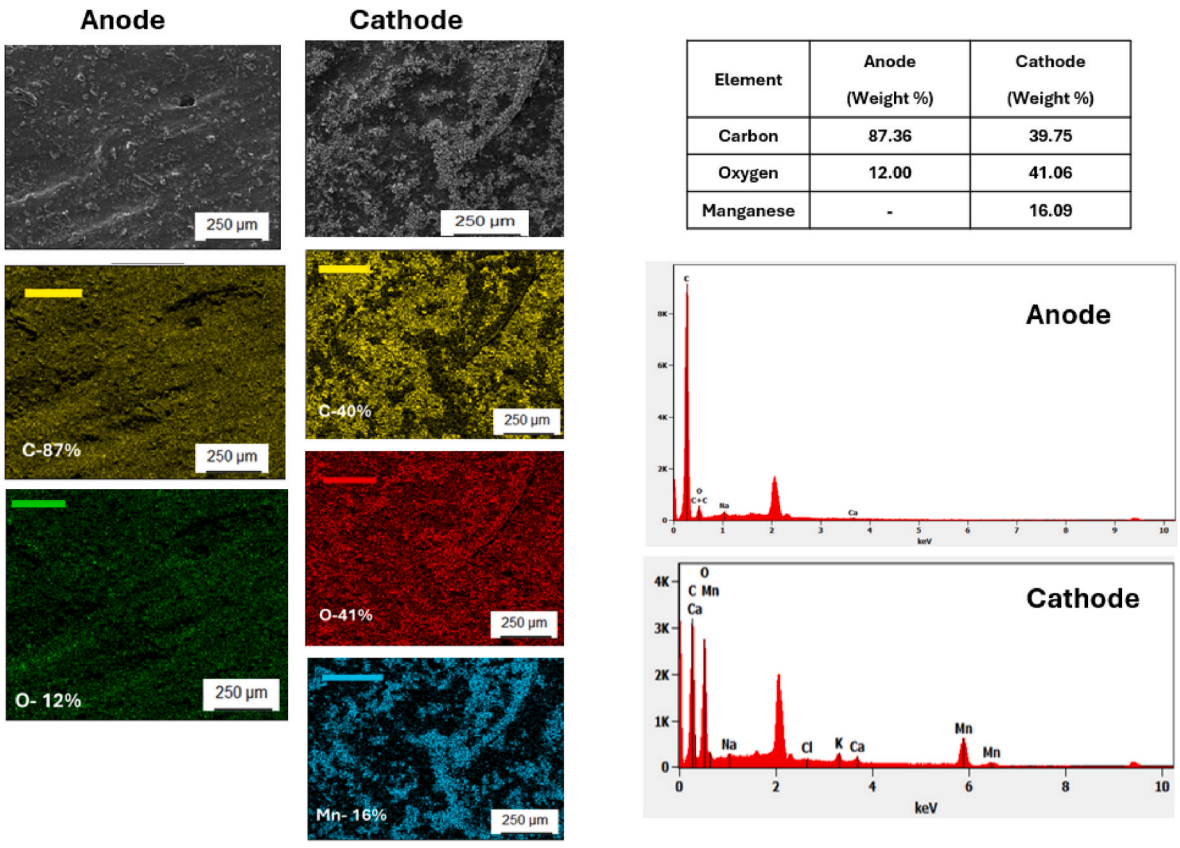

Element	Anode (Weight %)	Cathode (Weight %)
Carbon	87.36	39.75
Oxygen	12.00	41.06
Manganese	-	16.09

Fig. 4. EDX spectrum and elemental mapping of the anode shows carbon 87 % and Oxygen 12 %, whereas the cathode shows carbon of 40 %, Oxygen 41 % and Manganese 16 %.

motivated to further reduce the thickness of the membrane and anode. Further attempts are made to keep the membrane and anode thickness at 0.4 mm each. The membrane with 0.4 mm thickness is feasible to print as it gets the base support from the printing bed, whereas printing a 0.4 mm anode thickness layer results in inconsistent print even after keeping the solid top layer option active. The obvious reason for this inconsistency lies in the lack of base support provided by open reservoirs. Further attempts are made to keep membrane and anode thickness 0.4 mm and 0.6 mm, respectively, which results in consistent anode thickness. this is the final converged setup for the substrate with the reservoir thickness of 1 mm, which will be used in the rest of the experiment as discussed next.

An experiment is carried out to evaluate the wicking property or the solution storage capacity of the printed polymer substrate-based reservoir thickness of 1 mm, keeping the thickness of the membrane and the anode at 0.4 mm and 0.6 mm, respectively. The process starts once the printed specimen is soaked in water for 72 h to dissolve all the soluble materials and leave pores/voids for wicking behaviour. After 72 h, the specimens are removed from the water and completely dried in air for one day, and their weight is measured for three samples of every filament to calculate the margin of error. Once the weight is measured, dried samples are dipped into the water again and left for half an hour so that the water can be completely soaked. After that, the samples are removed from the water very gently, making sure no pressure is applied, avoiding any squeezing of the samples and the dripping of water droplets before measuring the weight of the samples. The difference in the weight of the wet and dry samples is calculated, which is tabulated in Table 2. Considering water density as 1 g/ml, the difference decides the amount of water in ml that the respective substrates can hold. Based on Table 2, Lay felt can hold the highest amount of water (0.5 ml), followed by Lay felt (0.492 ml), Lay form-60 (0.285 ml) and Lay form-40 (0.26 ml). Lay felt is the softest (spongy) among all four filament-based substrates, contributing to the highest water retention and holding properties.

Table 2
Water retention capacity of different printed filament-based substrates.

Filament	Dry (gms)	Wet (gms)	Difference (gms)
Lay fomm-40	0.589 ± 0.064	0.849 ± 0.073	0.26
Lay fomm-60	0.681 ± 0.013	0.966 ± 0.108	0.285
Lay felt	0.528 ± 0.048	1.028 ± 0.112	0.5
Gel lay	0.648 ± 0.017	1.14 ± 0.0946	0.492

Further, keeping the membrane and anode thickness 0.4 mm and 0.6 mm, OCV readings have been captured using a datalogger based on all four filaments, i.e. Gel lay, Lay felt, Layfomm-40, and Layfromm-60. The data gathered for three cycles is presented as shown in Fig. 5 These results indicate that the Gel lay option performs the best, offering a maximum OCV of 0.41 V, followed by Lay fomm-60 0.4 V, Lay felt 0.38 V, and Lay Fomm-40 0.32 V. Further, a stable OCV is obtained for around 1 h in every MFC setup. The functional component (backbone material) for Gel lay is polyamide, unlike the other filaments, which could be the reason for its better performance compared to the others. You et al. [21] have also shown that Gel-Lay material was the best choice from all the tested membranes due to its high-power generating performance, which is also proved to be true from the current study. Unlike the other three printed substrates, Lay felt does not allow the flow of the bacterial inoculum into the reservoir, and the probable reason is its structure after printing. A cross-section view is examined by cutting the sample longitudinally from the centre, as shown in Supplementary Fig. S3. The Gel lay-based substrates clearly show an anode layer and membrane and a void in-between, which represents the reservoir, whereas, in the case of Lay felt, all layers are stuck together, which causes bacterial inoculum to float on the top and cannot access the

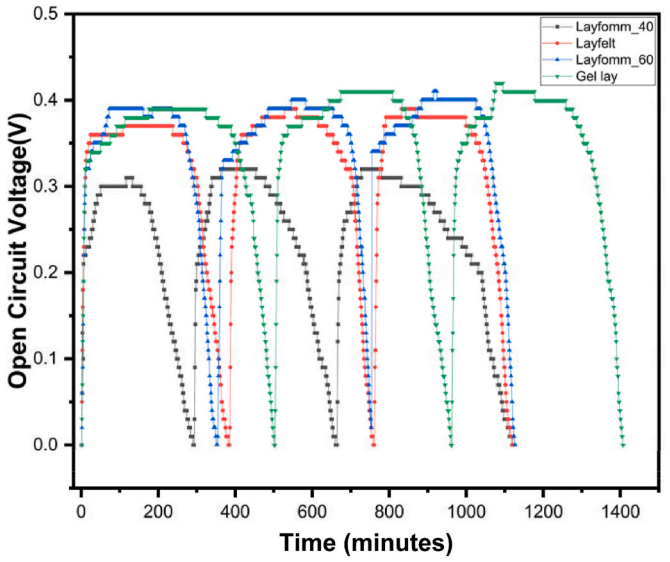

Fig. 5. Open circuit voltage representation of filament-based MFCs for three cycles having membrane and anode thickness of 0.4 mm and 0.6 mm (black) of all the four different filaments, i.e. Layfomm-40, Layfomm-60, Lay felt, and Gel lay.

internal structure of the substrates, rendering the performance to be inferior to Gel lay. Lay fomm-40 and Lay fomm-60 both revealed foamy microstructure. However, Lay fomm-60 substrates are more rigid and intact in their shape, which could be the reason for their better performance.

Further investigations are conducted to evaluate the effectiveness of membranes in all four filament substrates after the three cycles of OCVs are completed. The process starts with peeling off the layers of membranes facing the cathode side before the cathode-coated layer. These are the cathode surfaces facing the membrane, which are prepared for observing any bacterial attachment using SEM imaging. The samples for SEM are prepared by following an overnight protocol, as discussed in the materials and methods section, and the SEM images obtained are shown in Fig. 6. It can be observed that none of the substrates allowed the bacterial inoculum to cross to the cathode side, as there is no evidence of any bacterial attachment, which clearly indicates the effectiveness of all four membranes.

Whatman™ filter paper, which is generally used for making paper-based MFCs, generally has a thickness of less than 0.4 mm, and the electrode deposition is done on top of the paper, as presented by Jayapiriya et al. [6] where carbon nanotubes (CNT) of thickness 30 μm is deposited on the filter paper. Unlike filter paper, Porolay filaments offer mesoporous structures, which are developed after dissolvable material leaves a void after soaking in water. These mesoporous structures allow water-soluble electric paint to sweep inside due to the wicking property of the substrates. Thus, electrode coating is not just restricted to the top surface but can access the internal architecture of the raster path of printed substrates as well. This internally coated substrates-based anode allows more interaction with bacterial inoculum, more reaction sites, and subsequently, more electrons transfer to an external circuit. So, 30 μl of electric paint solution is dispersed on the anode side of 1 cm × 1 cm area using the crop casting method, and this is an additional coating done on top of screen coating, as discussed before. The cross-sectional view of the internally coated substrate is shown in Supplementary Fig. 4, which shows that the internal strands are covered with electric paint.

Electrical performance is evaluated in terms of OCV for three cycles of all four substrates based on the internal coating of printed strands, and the result is shown in Fig. 7. The results are similar to those in Fig. 5. However, the OCV values obtained are higher in this case for every filament substrate-based MFC. This higher OCV is attributed to the

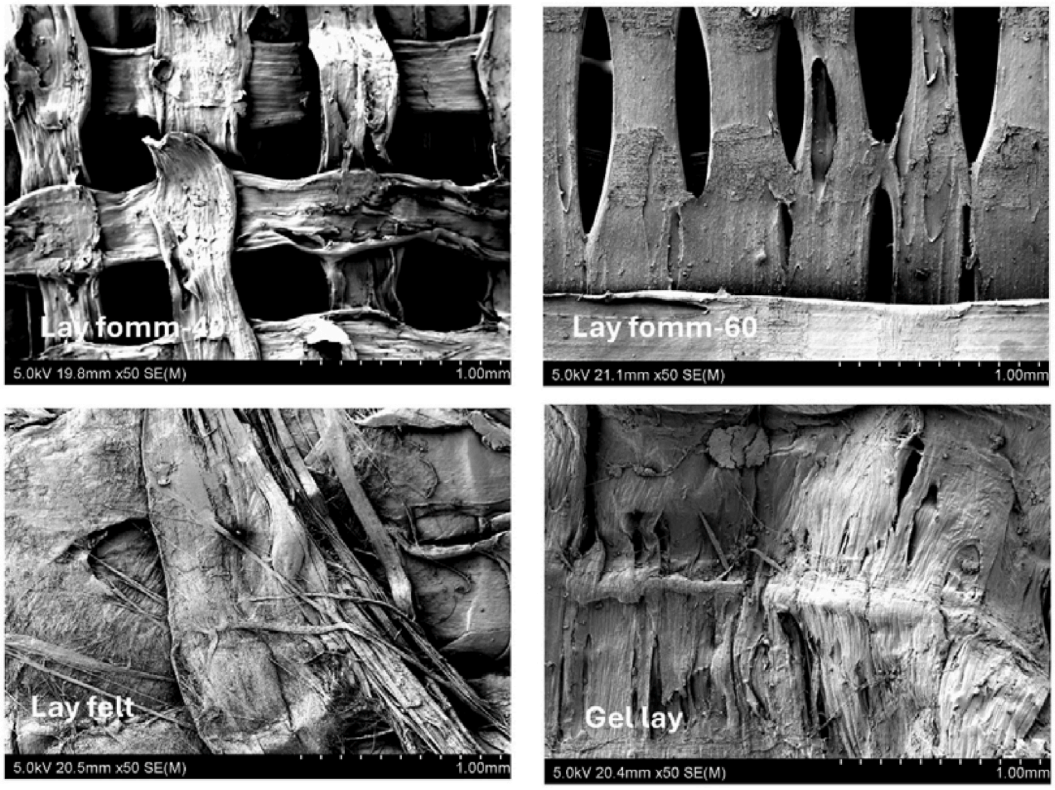

Fig. 6. SEM analysis of the membranes facing the cathode side for the effectiveness in terms of not allowing inoculum to cross the cathode side of all the four filament-based substrates.

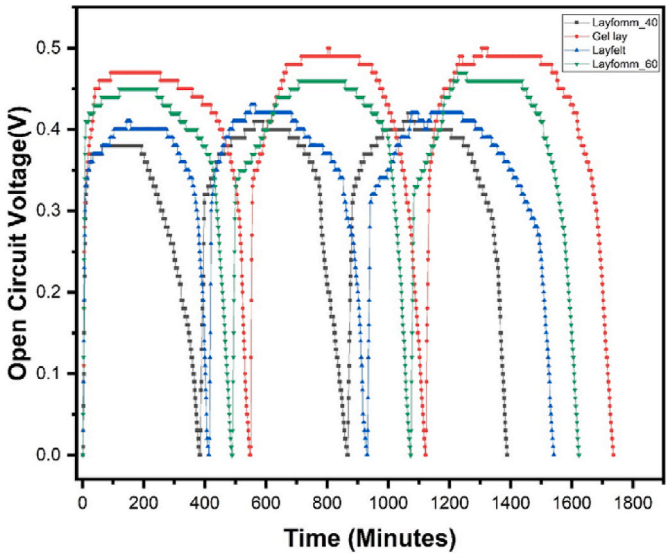

Fig. 7. Open circuit voltage representation of filament-based MFCs for three cycles with membrane and anode thickness of 0.4 mm and 0.6 mm (black) based on all the four different filaments, i.e. Layfomm-40, Layfomm-60, Lay felt, and Gel lay with surface and internally coated printed strands.

internal coating of the strands, which allows more electron-capturing abilities from bacterial inoculum which are then passed on to the external circuit. Controlled porosity is required for better performance in terms of better microbial attachment for an anode, and this is corroborated by the investigation done by Kumar et al. [24], where porous anode-based cells performed better in terms of OCV. Additionally, porous cathodes render more reaction sites. The Gel lay filament-based MFCs offer a maximum OCV of 0.49 V steadily for around 90 min, which is higher than the values with MFCs based on as-screen coated anodes, resulting in 0.41 V steadily for 60 min. Compared to an investigation done by Jayapiriya et al. [18], where a maximum OCV of 410 mV was obtained, the current study shows a maximum OCV of 490 mV. Further, in another study, Jayapiriya and Goel [18] achieved a stable OCV of 480 mV for 1 h, whereas the current results indicate a stable OCV of 490 mV for around 90 min. These improvements can be attributed to the mesoporous structure rendered possible by the printed filament-based substrates, allowing microbes to access the internally coated structures.

Once the MFCs maintain a steady OCV, power performance and polarisation curves are studied with the help of a load-controlled measurement technique, as discussed by Degrenne et al. [19], and the corresponding power and current curves are plotted for the setup of internally coated substrates as shown in Fig. 8. All the experiments are conducted thrice to ensure repeatability. The drop-casting internally coated strand-based Gel lay substrate MFCs generated a high maximum current density 93.9 μA/cm^2 with a maximum power density of 12.3 μW/cm^2, followed by 84.3 μA/cm^2 and 11.12 μW/cm^2, 73.2 μA/cm^2 and 8.55 μW/cm^2, 59.5 μA/cm^2 and 7.02 μW/cm^2 respectively for Lay fomm-60, Lay felt and Lay fomm-40. These results are synchronous with the maximum OCV for the respective substrates-based MFCs. Further, Gel lay-based MFCs results are comparable to Whatman filter paper grade 6 separator-based MFCs, which show the highest power density of 11.8 μW/cm^2 with a maximum current density of 91 μA/cm^2 [18]. This high value of current and power density obtained with Porolay series filaments are attributed to the mesoporous foamy structure offered by the printed filaments. This leads to more reacting sites for bacterial attachment. Furthermore, drop-cast electrode coating can impregnate the internal sites of fine-printed strands, shuttling more electrons to the external circuit and thereby reducing the mass transfer losses [25].

A comparative study was undertaken considering microbial fuel cells

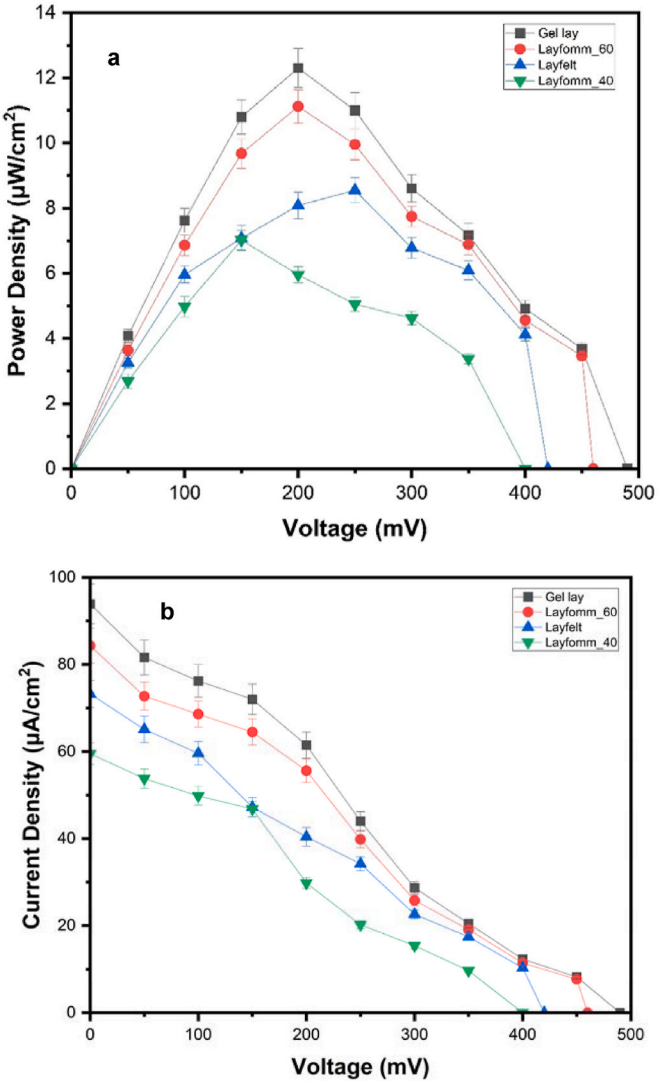

Fig. 8. Drop cast electrode-based MFCs showing (a) Polarisation curves, (b) Current density curves.

(MFCs) based on a Whatman filter paper (Grade 3) used for all critical components such as anode, reservoir, membrane and cathode. The reason for keeping the same filter paper for all components was to make better comparisons with monolithic printed MFCs. Further, electrode coating material (Electric paint) and other conditions were kept the same. The result showed a stable voltage (OCV) of 397 mV with a peak power density of 7.13 μW/cm^2. Compared to this, the polymer-based monolithic MFCs performed much better in terms of both OCV and peak power density responses. Furthermore, performance characterisation is represented in tabular form of different substrates (including Whatman grade 3) for better clarity in Table 3. This tabulated data

Table 3
Performance characteristics of different substrates-based MFCs.

Substrates	*Gel lay*	*LayFomm_60*	*Layfelt*	*LayFomm_40*	*Whatman (grade 3)*
current density (μA/cm$^{2)}$	93.9	84.3	73.2	59.5	61.3
Power density (μW/cm^2)	12.3	11.12	8.55	7.02	7.13
OCV (mV)	493	458	417	389	397

represents the mean value against each parameter.

3.3. Cost and simplicity analysis of monolithic Porolay series filament-based MFCs

Unlike the paper-based MFCs, where a different grade of Whatman™ filter paper is used for developing the critical components such as electrodes, reservoirs and separators, the current investigation uses a single filament to fabricate all critical components in a single-step printing. Further, the current study employs easy electrode-making processes such as screen printing and drop casting, which further reduce the complexity and cost involved. Considering the cost aspects, the price of polymer filament is USD 100/kg, the cost of electric paint is USD 30 (50 ml), MnO_2 nanoparticle is USD 25 (25 gm), and silver paste is USD 30 (10 gm). Considering all these costs, the price of a full-fledged, ready-to-use MFCs is less than USD 1.

4. Conclusion and future scopes

The current study utilised Porolay series filaments for the first time to develop monolithic polymer-based microbial fuel cells, replacing the filter paper, reported erstwhile. Further, this study shows how the membrane and the anode thicknesses affect the performance of microbial fuel cells (MFC). Various combinations of membrane thickness and anode thickness-based MFCs are investigated to evaluate their performance in terms of open circuit voltage (OCV). Further, four different filaments of the Porolay series are employed to characterise the performance of MFCs. It is found that an anode thickness of 0.6 mm and membrane thickness of 0.4 mm offer the best OCV of 0.41 V for Gel lay-based MFCs. Further, the drop-casting method is employed to develop the anode, where water-soluble electric paint impregnated and coated the fine-printed strands. This allowed microbial colonies to access more reacting sites and shuttle more electrons to the external circuit. It is further observed that drop casting-based MFCs offered a stable OCV of 0.49 V for about 90 min and delivered a power of 12.3 $\mu W/cm^2$ for Gel lay substrate-based MFCs. For the same level of Inoculum, the MFCs in the current study lasted almost 50 % more time compared to the paper based MFCs reported earlier. Additionally, more durable MFCs will be the subject of further research. It is also observed that further optimisation of the printed substrates is possible in terms of incorporating different architectures, which will improve more bacterial colony sites and, consequently, the cell performance. The design freedom of 3D printing to achieve complex intricate architecture can be further utilised top for further enhancing the reacting sites in both anode and cathode. Enhancing the reaction sites on the cathode side helps in improving catalytic activities, which subsequently will improve the overall performance of the cells.

CRediT authorship contribution statement

Vikash Kumar: Writing – original draft, Validation, Methodology, Investigation, Formal analysis, Conceptualization. **Sarat Singamneni:** Writing – review & editing, Supervision, Resources, Project administration, Funding acquisition, Conceptualization.

Declaration of competing interest

The authors declare the following financial interests/personal relationships which may be considered as potential competing interests: Sarat Singamneni reports financial support was provided by Royal Society of New Zealand. If there are other authors, they declare that they have no known competing financial interests or personal relationships that could have appeared to influence the work reported in this paper.

Acknowledgements

The authors wish to acknowledge a part of the support received from the Marsden Grant No. MFP AUT1901 in carrying out the research reported in this paper.

Appendix A. Supplementary data

Supplementary data to this article can be found online at https://doi.org/10.1016/j.renene.2025.122848.

References

[1] D. Nath, S. Kallepalli, L.T. Rao, S.K. Dubey, A. Javed, S. Goel, Microfluidic paper microbial fuel cell powered by Shewanella putrefaciens in IoT cloud framework, Int. J. Hydrogen Energy 46 (4) (2021) 3230–3239.
[2] M. Mohammadifar, J. Zhang, I. Yazgan, O. Sadik, S. Choi, Power-on-paper: origami-inspired fabrication of 3-D microbial fuel cells, Renew. Energy 118 (2018) 695–700.
[3] T.H. Nguyen, A. Fraiwan, S. Choi, Based batteries: a review, Biosens. Bioelectron. 54 (2014) 640–649.
[4] M. Puiu, V. Mirceski, C. Bala, Based diagnostic platforms and devices, Curr. Opin. Electrochem. 27 (2021) 100726.
[5] R. Veerubhotla, D. Das, D. Pradhan, A flexible and disposable battery powered by bacteria using eyeliner coated paper electrodes, Biosens. Bioelectron. 94 (2017) 464–470.
[6] U. Jayapiriya, S. Inoue, S. Goel, A facile technique to develop conductive paper based bioelectrodes for microbial fuel cell applications, Biosens. Bioelectron. 214 (2022) 114479.
[7] U.S. Jayapiriya, S. Goel, Influence of cellulose separators in coin-sized 3D printed paper-based microbial fuel cells, Sustain. Energy Technol. Assessments 47 (2021) 101535.
[8] Y.-F. Guan, F. Zhang, B.-C. Huang, H.-Q. Yu, Enhancing electricity generation of microbial fuel cell for wastewater treatment using nitrogen-doped carbon dots-supported carbon paper anode, J. Clean. Prod. 229 (2019) 412–419.
[9] M. Tanveer, T. Ambreen, H. Khan, G.M. Kim, C.W. Park, Based microfluidic fuel cells and their applications: a prospective review, Energy Convers. Manag. 264 (2022) 115732.
[10] A. Fraiwan, S. Mukherjee, S. Sundermier, H.-S. Lee, S. Choi, A paper-based microbial fuel cell: instant battery for disposable diagnostic devices, Biosens. Bioelectron. 49 (2013) 410–414.
[11] P. Rewatkar, P.K. Enaganti, M. Rishi, S. Mukhopadhyay, S. Goel, Single-step inkjet-printed paper-origami arrayed air-breathing microfluidic microbial fuel cell and its validation, Int. J. Hydrogen Energy 46 (71) (2021) 35408–35419.
[12] G. Oberoi, S. Nitsch, K. Janjić, H. Shokoohi-Tabrizi, A. Moritz, F. Moscato, E. Unger, H. Agis, The impact of 3D-printed LAY-FOMM 40 and LAY-FOMM 60 on L929 cells and human oral fibroblasts, Clin. Oral Invest. 25 (4) (2021) 1869–1877.
[13] A.A. Pitaru, J.-G. Lacombe, M.E. Cooke, L. Beckman, T. Steffen, M.H. Weber, P. A. Martineau, D.H. Rosenzweig, Investigating commercial filaments for 3D printing of stiff and elastic constructs with ligament-like mechanics, Micromachines 11 (9) (2020) 846.
[14] J.Z. Parrado-Agudelo, C. Narváez-Tovar, Caracterización mecánica de piezas de ácido poliláctico, policaprolactona y Lay-Fomm 40 fabricadas por modelado de deposición fundida, en función de los parámetros de impresión, Iteckne 16 (2) (2019) 111–117.
[15] V. Kumar, M.P. Behera, S. Singamneni, Polymeric microfluidic fuel cells with controlled printed patterns, 3D Print, Addit. Manuf. 11 (1) (2023) 78–93.
[16] M. Belka, L. Konieczna, M. Okońska, M. Pyszka, S. Ulenberg, T. Bączek, Application of 3D-printed scabbard-like sorbent for sample preparation in bioanalysis expanded to 96-wellplate high-throughput format, Anal. Chim. Acta 1081 (2019) 1–5.
[17] N.A. Kasim, W. Idris, K. Yusoh, Z. Ismail, Bare Conductive® role as filler in mechanical and electrical reinforcement of polyvinyl alcohol-based strain sensor. IOP Conference Series: Materials Science and Engineering, IOP Publishing, 2020 012111.
[18] U. Jayapiriya, S. Goel, Influence of cellulose separators in coin-sized 3D printed paper-based microbial fuel cells, Sustain. Energy Technol. Assessments 47 (2021) 101535.
[19] N. Degrenne, F. Buret, B. Allard, P. Bevilacqua, Electrical energy generation from a large number of microbial fuel cells operating at maximum power point electrical load, J. Power Sources 205 (2012) 188–193.
[20] V. Kumar, M.P. Behera, S. Singamneni, Microfluidic fuel cells printed with controlled rasterization, interdigitation, and multilevel honeycomb structures for better performance, 3D Print. Addit. Manuf. (2024).
[21] J. You, R.J. Preen, L. Bull, J. Greenman, I. Ieropoulos, 3D printed components of microbial fuel cells: towards monolithic microbial fuel cell fabrication using additive layer manufacturing, Sustain. Energy Technol. Assessments 19 (2017) 94–101.
[22] M.Z. Hussain, S. Khan, R. Nagarajan, U. Khan, V. Vats, Fabrication and microhardness analysis of MWCNT/MnO2 nanocomposite, J. Mater. 2016 (1) (2016) 6070468.

[23] S.A. Umoren, M.M. Solomon, V.S. Saji, Chapter 23 - other synthetic polymers, in: S. A. Umoren, M.M. Solomon, V.S. Saji (Eds.), Polymeric Materials in Corrosion Inhibition, Elsevier, 2022, pp. 541–563.
[24] V. Kumar, M.P. Behera, Y. Lv, B.P. Kamarajan, S. Singamneni, Hydrogen production from wastewater using interdigitated printed electrode-based Single-Chamber microbial electrolysis cells, Mater. Des. 245 (2024) 113237.
[25] X. Xie, L. Hu, M. Pasta, G.F. Wells, D. Kong, C.S. Criddle, Y. Cui, Three-dimensional carbon nanotube– textile anode for high-performance microbial fuel cells, Nano Lett. 11 (1) (2011) 291–296.